Relationships of interannual variability in SST and phytoplankton blooms with giant jellyfish (*Nemopilema nomurai*) outbreaks in the Yellow Sea and East China Sea

Yongjiu Xu[1], Joji Ishizaka[2], Hisashi Yamaguchi[3], Eko Siswanto[4], Shengqiang Wang[1]

[1]Graduate School of Environmental Studies, Nagoya University, Japan

[2]Hydrospheric Atmospheric Research Center, Nagoya University, Japan

[3]Earth Observation Research Center, Japan Aerospace Exploration Agency, Japan

[4]Research Institute for Global Change, Japan Agency for Marine-Earth Science and Technology, Japan

Corresponding author: Joji Ishizaka (jishizak@hyarc.nagoya-u.ac.jp)

Keywords: interannual variability, SST, satellite chlorophyll, jellyfish, outbreak

Abstract Giant jellyfish (*Nemopilema nomurai*) outbreaks in relation to satellite sea surface temperature (SST) and chlorophyll-*a* concentrations (Chl-*a*) were investigated in the Yellow Sea and East China Sea (YECS) from 1998 to 2010. Temperature, eutrophication, and match–mismatch hypotheses were examined to explain long-term increases and recent relaxations of *N. nomurai* outbreaks. We focused on the timing of SST reaching 15°C, a critical temperature enabling polyps to induce strobilation and allowing released ephyra to grow. We analyzed the relationship of the timing with interannual variability of SST, Chl-*a*, and the timing of phytoplankton blooms. Differences in environmental characteristics among pre-jellyfish years (1998–2001), jellyfish years (2002–2007, 2009), and non-jellyfish years (2008, 2010) were assessed on this basis. The SST during late spring and early summer increased significantly from 1985 to 2007. This indicated that high SST is beneficial to the long-term increases in jellyfish outbreaks. SST was significantly lower in non-jellyfish years than in jellyfish years, suggesting that low SST might reduce the proliferation of *N. nomurai*. We identified three (winter, spring, and summer) major phytoplankton bloom regions and one summer Chl-*a* decline region. Both Chl-*a* during non-blooming periods and the peak increased significantly from 1998 to 2010 in most of the YECS. This result indicates that eutrophication is beneficial to the long-term increases in jellyfish outbreaks. Timing of phytoplankton blooms varied interannually and spatially, and their match and mismatch to the timing of SST reaching 15°C was not corresponded to the long-term increases in *N. nomurai* outbreaks and the recent absence.

1 Introduction

The Yellow Sea and East China Sea (hereafter YECS), the largest continental marginal seas in the western North Pacific Ocean (Jiao et al. 2007), are surrounded by China, Korea, and Japan (Fig. 1). They are connected to the Pacific Ocean, the South China Sea, and the Sea of Japan by the strait between Taiwan and the Ryukyu Islands, the Taiwan Strait, and the Tsushima Strait, respectively. YECS areas are highly dynamic with a variety of distinguishable water masses. The area is characterized by a wide continental shelf (<200 m depth) and extremely dynamic seasonal river runoffs (Zhang et al. 2007; Siswanto et al. 2008). The freshwater runoffs, especially from the Changjiang River, and oceanic currents, such as the Kuroshio and Taiwan warm currents, induce major circulation patterns in the YECS. The Changjiang estuary (CJE) and its adjacent YECS waters are highly productive and resource-rich (Beardsley 1985). However, this ecosystem is also sensitive to variations in runoff from the Changjiang River, which has been undergoing long-term modifications due to human activities such as the use of chemical fertilizers, dam construction, and land modification (Gao and Song 2005; Li et al. 2007; Kim et al. 2009). Dissolved inorganic nitrogen levels have been increasing in the YECS since the 1980s, as influenced by the Changjiang River Discharge (Siswanto et al. 2008), terrigenous nitrogen fertilizer utilization (Wang 2006), and coastal aquaculture (Hu et al. 2010). Eutrophication due to increased nutrients has generated more frequent algal blooms in Chinese coastal waters since the 1990s (Tang et al. 2006).

Nemopilema nomurai, one of the largest jellyfish species in the world, is distributed mainly in the East Asian marginal seas, including the Bohai Sea (BS), the Yellow Sea, the East China Sea, and the Sea of Japan (Kawahara et al. 2006; Uye 2008).

Massive outbreaks of *N. nomurai* have historically been extremely rare, occurring approximately once every 40 years, in 1920, 1958, and 1995 (Yasuda 2004; Uye 2011). However, since 2002, outbreaks of *N. nomurai* have become more frequent and more extensive across YECS areas, occurring every year except 2008, 2010, and 2011 (Fisheries Research Agency, Japan: http://jsnfri.fra.affrc.go.jp/Kurage/kurage_top.html; accessed 18 March 2012). Previous studies have suggested that anthropogenic environmental changes such as eutrophication, habitat modification, overfishing, and global warming are responsible for these recent outbreaks (Purcell et al. 2007; Uye 2008, 2011). *N. nomurai* has a complex life cycle, with alternate sexual and asexual stages. The abundance of jellyfish reflects the success of excysting during the podocyst stage and the production of ephyrae in the polyp stage (Kawahara et al. 2006; Purcell et al. 2009; Kawahara et al. 2013). Judging from the occurrence of young medusae, Kawahara et al. (2006) speculated that the strobilation of polyps occurs in late spring to early summer in the YECS. During a recent survey, ephyrae were found for the first time in the northwestern East China Sea, and detachment from polyps was estimated to have occurred in early May near the mouth of the Changjiang River and along the coast of Jiangsu Province (Toyokawa et al. 2012).

To determine the driving factors behind the recent outbreaks in *N. nomurai*, we examined three hypotheses (temperature, eutrophication, and match–mismatch) during the ephyral stage in YECS. Temperature increases raise the physiological rates of both phytoplankton and the herbivorous zooplankton that feed on them (Sommer and Lengfellner 2008). With more jellyfish appearing in warmer years, temperature-related effects could become evident in polyp strobilation and ephyral growth (Richardson et al. 2009). In laboratory experiments, warm temperatures have been confirmed to increase

polyp strobilation and ephyral growth in *N. nomurai* (Kawahara et al. 2006). A temperature of 15ºC is critical, allowing released ephyrae to grow (S. Uye, personal communication) and producing the highest cumulative strobilation rate for *N. nomurai* (Kawahara et al. 2013).

Eutrophication due to increased nutrient input may increase the phytoplankton biomass, which may further enhance zooplankton production to supply more food to jellyfish (Uye 2008; Purcell 2012). Additionally, eutrophication could cause more frequent flagellate-phytoplankton blooms. Changes in the food web may reduce the size of the zooplankton community, leading to more favorable conditions for jellyfish than for fish (Purcell et al. 2007; Richardson et al. 2009; Purcell 2012). Moreover, eutrophication with enhanced organic matter production may contribute to the frequent occurrence and greater intensity of hypoxia/anoxia in coastal waters (Chai et al. 2006), which would probably benefit jellyfish rather than fish (Purcell 2012).

The match–mismatch hypothesis predicts that the growth and survival of the larvae of marine predators depends on a temporal match with prey availability (Cushing 1990; Durant et al. 2005). A number of studies have indicated that top predators (e.g., jellyfish, fish) are indirectly controlled by primary production via bottom-up processes, and this hypothesis seems to be applicable for a wide range of marine predators (Frank et al. 2007; Gremillet et al. 2008).

Satellite-detected sea-surface temperatures (SST) and ocean color (Chl-*a*) have been used to characterize physical and ecosystem features, respectively, in the YECS (Hickox 2000; Yamaguchi et al. 2012, 2013). These satellite monitoring data are useful to monitor eutrophication and harmful algal blooms (Ahn and Shanmugam 2006; Yamaguchi et al. 2013). Due to the large spatial scales of giant jellyfish distributions,

traditional oceanographic observations would be difficult to apply in this kind of study; instead, satellite images of SST and Chl-*a* are useful for detecting environmental variables related to jellyfish outbreaks. The Chl-*a* is also expected to serve as an indicator of zooplankton abundance (i.e., food for jellyfish) (Gremillet et al. 2008).

The objective of this study was to test the three hypotheses (temperature, eutrophication, and match–mismatch) using satellite SST and Chl-*a* data. Interannual variability in spring and early summer (March–June) SST were investigated, and interannual variability in the timing and magnitude of phytoplankton blooms were compared with the timing of SST reaching 15°C (hereafter Tsst15). In the following sections, we described the environmental characteristics during pre-jellyfish years (PJY, 1998–2001), jellyfish years (JY, 2002–2007, 2009), and non-jellyfish years (NJY, 2008, 2010), and discuss the factors controlling the outbreak of giant jellyfish.

2 Materials and methods

2.1 SST dataset

The SST data used in the present study were 8-day averaged (hereafter 8-day weekly) and monthly nighttime, 4-km resolution data from Pathfinder version 5 AVHRR/NOAA (Advanced Very High Resolution Radiometer) for 1998–2002 and from MODIS/AUQA (Moderate Resolution Imaging Spectroradiometer) Level 3 for 2003–2010 (Table 1). The AVHRR and MODIS data were screened for quality control. Only pixels with quality levels of 4–7 were used (http://www.nodc.noaa.gov/SatelliteData/pathfinder4km/userguide.html) as well as level 0 data (http://oceancolor.gsfc.nasa.gov/DOCS/modis_sst/). We used the combined 8-day weekly/monthly datasets (1998–2010) for further study, as the accuracy of the MODIS

SST data was consistent with the AVHRR Pathfinder SST fields (Minnett et al. 2002).

2.2 Ocean color dataset

Daily remote sensing reflectance data from two sensors, the Sea-viewing Wide Field-of-view Sensor (SeaWiFS) and MODIS/Aqua, were obtained from the NASA Goddard Space Flight Center (http://oceancolor.gsfc.nasa.gov/). Remote sensing reflectance (*Rrs*) at wavelengths of 412, 443, 490, and 555 nm [Rrs(412), Rrs(443), Rrs(490), Rrs(555)] from SeaWiFS and at 412, 443, 488, and 547 nm [Rrs(412), Rrs(443), Rrs(488), Rrs(547)] from MODIS were analyzed. Several different datasets with various reprocessing versions and levels were used (Table 1).

We used empirical Yellow Sea Large Marine Ecosystem Ocean Color Work Group (hereafter YOC) Chl-*a* algorithms for the study area from the SeaWiFS Reprocessing 5.1 (R2005.1) dataset developed by Siswanto et al. (2011). A normalized water-leaving radiance value of 555 nm [nLw(555)] was used to switch from the non-turbid standard algorithm to the turbid algorithm (details in the Appendix). Yamaguchi et al. (2013) modified this switch to produce a smooth image with a linear combination of these algorithms for the low value of nLw(555). Because the YOC Chl-*a* algorithm was based on an older SeaWiFS R2005.1 dataset and a newer SeaWiFS Reprocessing 2010.0 (R2010.0) dataset is available, linear conversions between the datasets were conducted using band ratios [Rrs(412)/Rrs(490) and Rrs(443)/Rrs(555)]. Furthermore, to make the long time series from SeaWiFS (1998–2010) and MODIS (2002–2010) consistent with one another, we conducted linear conversions of MODIS-Aqua Reprocessing 2009.1/2010.0 (R2009.1/R2010.0) band ratios [Rrs(412)/Rrs(488) and Rrs(443)/Rrs(547)] to SeaWiFS band ratios [Rrs(412)/Rrs(490) and Rrs(443)/Rrs(555)]

(details in the Appendix).

To make the 4-km resolution SeaWiFS R2010.0 Level 2 GAC datasets compatible with the 1-km MODIS R2009.1/R2010.0 Level 2 LAC datasets, MODIS data were reduced by four times by averaging four neighboring pixels into one and remapping them to the same dimensions as SeaWiFS (386 × 386 pixels for 17° × 17° in YECS). The newly processed MODIS and SeaWiFS daily datasets were then merged to make more consistent and cloud-free long-term 8-day weekly and monthly Chl-*a* datasets. All merged Chl-*a* data were re-binned to 1° × 1° to reduce the influence of meso-scale variability. We used relatively loose criteria to exclude outliers caused by cloud-edge effects (Vantrepotte and Melin 2009). First, we selected the median value in each grid. Second, assuming a lognormal distribution for the 13-year 8-day weekly and monthly Chl-*a* data in all grids, we removed outliers by excluding data points that were greater than three standard deviations from the mean. These processes enabled 144 ocean grid points to each have data for a 612 8-day weekly time series (14 8-day weeks for 1997 and 598 8-day weeks for 1998–2010). All data processing was conducted using NASA SeaDAS software (version 6.2) and Windows Image Manager (WIM) software (http://www.wimsoft.com/).

2.3 Gaussian fitting for phytoplankton blooms

The middle area of the temperate YECS is characterized by a typical spring bloom and a modest fall bloom (Furuya et al. 2003), while the coastal area of the YECS is characterized by a long-duration bloom from spring to autumn (Yamaguchi et al. 2013), and the subtropical area of the Kuroshio is characterized by winter phytoplankton increases (Wang et al. 2010). A flexible curve-fitting procedure was used to model these

blooms. First, a modified Gaussian function, which has been widely used to model time series of satellite-derived Chl-*a* (Yamada and Ishizaka 2006; Platt et al. 2007; Zhai et al. 2011), was selected for the period from winter to summer, when polyp strobilation and larval growth are expected.

Second, the Chl-*a* time series for winter, spring, and summer blooms were selected for fitting. We did not take into account the possible fall bloom because it was not relevant to the analysis of young jellyfish. The Chl-*a* time series was adjusted for each grid so that the largest seasonal blooms would be at the center of each respective time series. Thus, the periods from August 29 to August 28 of the following year, January 1 to July 30, and January 1 to December 31 were used to detect winter, spring, and summer blooms, respectively.

Third, the 8-day weekly time series for Chl-*a*, *CHL(t)*, over one year or half a year were fitted to a modified Gaussian function as follows:

$$CHL(t) = B_s \cdot t + B_i + a \cdot \exp\left\{-\left[\frac{(t-t_p)^2}{2\sigma^2}\right]\right\},$$

where B_s and B_i are the baseline slope and intercept, respectively. $B_s \cdot t + B_i$ and $B_s \cdot t_p + B_i + a$ are baseline and peak Chl-*a*, and t_p, $t_p - 2\sigma$, and $t_p + 2\sigma$ are the times of peak, start, and end of phytoplankton bloom, respectively. The tilted baseline for phytoplankton blooms was used because Chl-*a* before and after the bloom during the analysis periods were significantly different in most of the grids (W-R test: h = 1, $p < 0.1$, at a 90% confidence level, data not shown). Non-bloom Chl-*a* was defined as the average Chl-*a* of before and after the bloom during the analysis period.

Fourth, for each year in each grid, three types of bloom time series were fitted to

the modified Gaussian function described above using the nonlinear least-squares method. If the number of valid values of the time series was less than half of the number for the whole period (<12 8-day weeks for the time series of January 1 to July 30, <22 8-day weeks for the time series of August 29 to August 28 of the following year, and January 1 to December 31), this time-series was removed from the fitting. The quality of the three types of time-series fittings in each grid was assessed using determination coefficients, and the best bloom type was chosen. In some grids, the fitted curve with one negative peak with highest determination coefficient was found. This region was defined as phytoplankton decline region. We were unable to analyze data for a few years in some areas with low determination coefficients ($R^2 < 0.5$).

Fifth, the average timings of phytoplankton blooms for climatological time series from 1998 to 2010 were also fitted the same way, except for the time series of August 29 to August 28 of the following year and January 1 to December 31. For the fitting, B_s was set as 0 (non-tilted baseline) because the difference of Chl-*a* between before and after the bloom during analysis periods was not significant (W-R test: h = 0, $p > 0.1$, at a 90% confidence level, data not shown).

2.4 Statistical analysis

One-sided Wilcoxon rank-sum (W-R) tests (Michael and Proschan 2010) were used to compare SST in JY and NJY, and two-sided W-R tests were used to compare SST in JY and PJY. Linear regression analysis with year was used to obtain long-term trends in monthly SST, non-bloom Chl-*a*, and peak Chl-*a*.

We first identified geographical regions based on Chl-*a* peaks from the Gaussian fitting. Then, to further discriminate spring and summer bloom regions with the

geographical and climatological differences in temporal patterns of Chl-*a*, we conducted K-means clustering analysis based on parameters of the phytoplankton bloom (start time, end time, peak time, baseline Chl-*a*, and peak Chl-*a*) (Henson and Thomas 2007). This analysis was performed on composites of the 13-year climatological 8-day weekly Chl-*a* time series on the basis of silhouette values (Kaufman and Rousseeuw 1990). These values indicated that the optimum number of clusters for further separation was seven. All statistical analyses and model fitting were performed in MATLAB2012 (www.mathworks.com)

3 Results

3.1 SST seasonality during 1998–2010

Coastal and middle areas between China and Korea were characterized by large seasonal variations in SST, likely because these areas are shallow and subjected to large quantities of river runoff. The waters of the southeast YECS were characterized by relatively small seasonal variations in SST, dominated by the warm Kuroshio Current. In winter, the 15°C water was distributed from the Taiwan Strait northeastward along the Zhejiang-Fujian coast (Fig. 2a), displaying a distribution pattern similar to that of the tongue-shaped front off the CJE. The 15°C water was found in the center of the YECS, from the northern coast of the CJE to offshore in spring (Fig. 2b). SST was quite uniform in the YECS in summer, and higher than 15°C throughout the study region (Fig. 2c). In fall, 15°C water was observed from east of the Shangdong Peninsula to south of Korea (Fig. 2d).

3.2 Interannual variability in SST

We selected seven areas to represent the whole YECS, according to geographic characteristics, not including the Kuroshio and offshore waters where SST was always near or above 15ºC. These areas were distributed from the Chinese and Korean coasts to the middle of the YECS and included the BS, the middle of the northern Yellow Sea (MNYS), the Chinese coast of the southern Yellow Sea (CSYS), the coast of the Shangdong Peninsula (CSDP), the middle of the southern Yellow Sea (MSYS), the Korean coast of the southern Yellow Sea (KSYS), and the CJE (Fig. 1).

Interannual variability in SST for all areas in the YECS was approximately 0–5°C during spring to summer, and smaller than the seasonal variability (Fig. 3). SST decreased significantly ($r < –0.5$, $p < 0.05$) in April, May, and June in the MSYS from 1998 to 2010 (Fig. 3e). A significant decrease ($r < –0.5$, $p < 0.05$) was also observed in March, May, and June in the CSDP (Fig. 3d); however the decrease was only significant in March, May, and June in the CSYS, MNYS, and BS, respectively (Fig. 3a-c).

The SST was much lower in NJY than in PJY and JY from spring to early summer, with differences of approximately 0–5°C (Fig. 4). However, the differences in SST in JY and PJY were not significant (W-R test: h = 0, p > 0.1, at a 90% confidence level) in most of the YECS. The range of the differences was approximately 0–1.5°C from spring to early summer. Longer time series (1985–2007, data not shown) with additional SST datasets from AVHRR showed significant increase ($r > 0.5$, $p < 0.05$, 1.50ºC) during the 23 years in the majority of the YECS (MSYS, CSYS, CJE, MNYS and BS) throughout spring and early summer. The low SST in NJY caused the significant decrease from 1998 to 2010 in the YECS. The long-term results indicate that the SST increased significantly with a maximum in PJY and JY during spring and early summer in recent decades.

The spatial distribution of the SST difference between JY and NJY also indicates that SST in NJY was lower than in JY in large areas of YECS from April to June (Fig. 5). In March, SST in NJY was only slightly lower (0–1.5°C) than in JY, and the difference was not statistically significant at a 90% confidence level (h = 0, $p > 0.1$) throughout the YECS, except in two grids (Fig. 5a). In April, SST in NJY was significantly lower (2–5°C) than in JY (W-R test: h = 1, $p < 0.1$) in CJE and its adjacent waters (Fig. 5b). In May, SST in NJY was significantly lower (1.5–2°C) than in JY in a large area of the YECS, including the CSYS, MSYS, and Huanghe River estuary of the BS (Fig. 5c). In June, SST in NJY was significantly lower (2–3°C) than in JY (h = 1, $p < 0.1$) in most parts of the BS, CSYS, MSYS, and KSYS (Fig. 5d).

3.3 Phytoplankton bloom climatology

Based on the seasonal peaks in Chl-*a*, we identified three (winter, spring, and summer) major bloom regions and one summer decline region in the YECS (Fig. 6a). The winter bloom region was distributed in the southeast subtropical region with low seasonality, influenced by the Kuroshio. The spring bloom region covered most of the YECS, specifically in the middle regions deeper than 50 m. The summer bloom region mainly occupied the coastal area of the YECS, with the boundary corresponding well with the 50-m isobath, extending from the coast of Fujian Province to most of the BS and the Korean coast. The summer decline region was confined to the coast of Shangdong Peninsula.

In the winter bloom region, seasonal and interannual variability of Chl-*a* was small (Fig. 7a), with the lowest baseline (< 0.1 mg m^{-3}) and peak (< 0.25 mg m^{-3}). In the spring bloom region, seasonality was larger, with the tilted baseline and peak of 0.5–0.7

and 1.2 mg m^{-3}, respectively (Fig. 7b). Chl-*a* in coastal regions of the YECS exhibited a distinct seasonal cycle, with a peak in midsummer. The baseline and peak in coastal regions were highest, with values of 1.8 and 3.1 mg m^{-3}, respectively (Fig. 7c). The interannual variability of Chl-*a* in the summer bloom region, represented by standard deviations (0.23–0.73 mg m^{-3}), was large around the peak of the bloom. In the summer decline region, the peak was negative with a fitted Gaussian function (Fig. 7d).

The start time of the summer bloom was late in the CJE, CSYS, and BS in May or June (Fig. 8a). The end time of the winter and spring blooms was from May to June around the Okinawa Islands and March to April in the middle of YECS (Fig. 8b). In the coastal regions, the end of the bloom occurred from early September in the CSYS to late November in the CJE, BS, and KSYS. The peak of the phytoplankton bloom generally occurred in mid-January for most of the southeast, in early or mid-April for the middle of the YECS, and in late July or early August for the coast of the YECS (Fig. 8c). In the subtropical Okinawa region, a long and low-intensity winter increase in Chl-*a* was observed (Fig. 8d, f). In contrast, bloom duration tended to be shorter in the middle YECS compared with other regions (Figs.7b, 8d). Non-bloom Chl-*a* were extremely low in the Okinawa region and generally high in the middle and coastal regions of the YECS, with a maximum in BS (Fig. 8e). High peak (>4 mg m^{-3}) was found in CJE and its adjacent waters, CSYS, KSYS, and in most parts of the BS (Fig. 8f).

3.4 Interannual variability in the timing of phytoplankton blooms and the Tsst15

We focused on the YECS where SST varied around 15°C and excluded the Kuroshio and offshore waters (Fig. 6b). A cluster analysis of the 13-year Chl-*a* time

series data revealed seven distinctive regions with significant different seasonal cycles of Chl-*a*; BS, MNYS, CSYS, CSDP, MSYS, KSYS, and CJE. The same abbreviated names were used for each region as the name of the SST study because the areas of investigated SST in Section 3.2 were located near the centers of each region (Fig. 1).

A high summer peak with a long bloom period was observed for most of the years in the BS, CSYS, KSYS, and CJE (Fig. 9, Table 2). A lower Ch-*a* during shorter spring bloom was observed in the majority of the years in MNYS and MSYS. The Chl-*a* peak was negative in midsummer in the CSDP. Significant increases ($r > 0.5$, $p < 0.05$) in both non-bloom and peak Chl-*a* from 1998 to 2010 were observed in most regions of the YECS (Fig. 9, Table 2). The increases in non-bloom and peak Chl-*a* were 55.0, 35.8, 18.0, 35.7% and 80.0, 60.0, 55.0, 38% in BS, CSYS, MSYS, KSYS, respectively. Both non-bloom and peak Chl-*a* also increased in the CJE (9.5 and 8–10%, respectively).

The start and end times of the blooms exhibited considerable interannual variability (more than six 8-day weeks) in BS, CSYS, KSYS, and CJE (Fig. 9, Table 2). The timing of phytoplankton blooms exhibited less interannual variability (within six 8-day weeks) in MNYS and MSYS. In the CSDP, the start and end times of the phytoplankton decline exhibited considerable interannual variability (more than six 8-day weeks). The Tsst15 exhibited similar interannual variability in almost all regions, generally within two 8-day weeks: this was near the start of the bloom in the BS, CSYS, KSYS, and CJE regions, and near the end of the bloom in the MNYS and MSYS regions in most years (Fig. 9, Table 2). The Tsst15 was also close to the start of the phytoplankton decline in the CSDP in all years (Fig. 9d).

4 Discussion

In this study, three hypotheses (temperature, eutrophication, and match–mismatch) were examined to explain the jellyfish outbreaks after 2002, and their absence in 2008 and 2010, using satellite SST and Chl-*a*.

4.1 Temperature hypothesis

Global warming is considered an important factor affecting increases in jellyfish outbreaks (Purcell et al. 2007; Richardson et al. 2009). Our analysis indicated that SST significantly increased during the 23 years from 1985 to 2007 in spring and early summer. This finding was consistent with previous results, such as those published by Lin et al. (2005), who observed that the regional mean temperature in the Yellow Sea increased by 1.7ºC from 1976 to 2000. The maximum SST in PJY and JY indicated that the long-term increase in SST generally corresponded to recent increases in jellyfish outbreaks.

Uye (2008) speculated that warmer temperatures may induce higher birth rates of *N. nomurai* medusae by accelerating asexual reproduction, based on the results of laboratory experiments (Kawahara et al. 2006). Our analysis of the SST in YECS based on satellite data also indicated that the high temperature in YECS was favorable for *N. nomurai*. This result supports the temperature hypothesis.

The temperature hypothesis can also explain the lack of *N. nomurai* outbreaks in 2008 and 2010 (NJY), when the SST was as low as in the 1980s. Because *N. nomurai* has a short lifespan (one year), the fluctuation of abundance could be caused by short-term climatic variations, as has been suggested for *Aurelia aurita* and *Cyanea lamarckii* in the North Sea (Lynam et al. 2004, 2005). The absence of *N. nomurai* outbreaks in 2008 and 2010 may be attributable to unfavorable conditions caused by the low temperatures associated with the climate variation. However, no jellyfish outbreak

occurred in PJY, even though the SST was as high as in JY. This indicates that high temperature conditions are necessary but not sufficient for jellyfish outbreaks.

4.2 Eutrophication hypothesis

Our results revealed that both the non-bloom and peak Chl-*a* increased significantly from 1998 to 2010, with a great increase observed in coastal regions (Fig. 9, Table 2). This indicates that eutrophication was more severe in recent years (JY and NJY), as the nutrient loading continued from land (Zhou et al. 2008; Gao and Zhang 2010). The high food availability resulting from more eutrophic conditions in coastal regions of the YECS, especially in the CSYS, KSYS, and BS, may favor polyp strobilation and survival of ephyra in JY. Conversely, less eutrophic conditions limit polyp strobilation, likely resulting in lower survival of ephyra and thus less recruitment of *N. nomurai* medusae in PJY.

However, high eutrophic conditions in NJY did not correspond to high jellyfish abundance, indicating that eutrophication was necessary but not sufficient for jellyfish outbreaks. As explained in Section 4.1, the low temperature is a probable cause of unfavorable conditions for *N. nomurai* even in a eutrophic environment.

Kawahara et al. (2006) speculated that the ecosystem changes associated with eutrophication may be responsible for the enhancement of giant jellyfish populations. We found that phytoplankton, which is food for zooplankton, increased significantly from PJY to JY in YECS. This result indicates that the ecosystem is changing in YECS associated with eutrophication (Kawahara et al. 2006; Siswanto et al. 2008). The increase in phytoplankton due to eutrophication in combination with higher temperatures due to climate change probably led to long-term increases in jellyfish

outbreaks.

4.3 Match–mismatch hypothesis

High temperatures may act directly on polyps to enhance strobilation (Kawahara et al. 2006). Alternatively, several studies suggested an indirect influence of temperature through alteration of the timing of phytoplankton blooms to synchronize with the period of rapid ephyral growth (Båmstedt et al. 2001; Lynam et al. 2004). We found that the ephyral stage, as indicated by the Tsst 15, was always near the start of the bloom in coastal areas, while it was always near the end of bloom in middle areas. Furthermore, variability in the start and end times of phytoplankton blooms did not correspond to timings of the ephyral stage in warmer JY and colder NJY in each region. In particular, the delay in the Tsst15 did not result in a mismatch with phytoplankton blooms in NJY. A change in the physiology of jellyfish larvae due to low SST was more likely to have resulted in low survival of ephyra in NJY (Uye 2008; Purcell et al. 2009).

Our analyses also indicated that the timing of phytoplankton seasonal blooms differed greatly between coastal and middle areas (Fig. 9). If the timing of phytoplankton blooms corresponds to jellyfish prey abundance, matches and mismatches between the timings of phytoplankton blooms and the Tsst15 were observed in all years in the coastal (BS, CSYS, KSYS, and CJE) and middle (MNYS and MSYS) areas of the YECS, respectively (Fig. 9). The difference indicates that survival of ephyra may differ between middle and coastal regions, although no information is available at present.

The main prey of *N. nomurai* medusae are small copepods and gastropod larvae (size <1 mm) that may directly feed on phytoplankton (Uye 2008). According to Lee et

al. (2008), the ephyrae of *N. nomurai* could feed on prey similar to that of large adult medusae. Thus, the timing of phytoplankton blooms may affect survival of ephyra through a complex bottom-up process (Gremillet et al. 2008). In general, a time lag occurs between phytoplankton blooms and increases in zooplankton abundance (Kiorboe and Nielsen 1994; Zervoudaki et al. 2009).

Kang et al. (2012) suggested that copepod abundance increases from spring until the seasonal peak in summer along the Korean western coast, increases from February with the seasonal peak in April, and then decreases until August in the north East China Sea near the Tsushima Strait. If we assume that the results of Kang et al. (2012) in the Korean coast and in the northern East China Sea are applicable to the YECS coastal and middle regions, the Tsst15 (ephyral stage) corresponded to the copepod abundance peak in coastal regions and the minimum in the middle regions. This is consistent with our results for phytoplankton blooms: match and mismatch in coastal and middle regions, respectively. However, Kang et al. (2012) only investigated average bimonthly zooplankton data from February to December in Korean waters. Temporal and spatial data limitations obviously restrict interpretation of the match–mismatch between zooplankton abundance and the jellyfish ephyral stage. More *in situ* data are required to validate the details of the match–mismatch of *N. nomurai* to prey abundance.

5 Conclusions

Using 13 years of satellite (AVHRR, SeaWiFS, MODIS-Aqua) SST and Chl-*a* data, we characterized long-term environmental variables related to interannual variability of *N. nomurai* outbreak in the YECS for the first time. Three hypotheses (temperature, eutrophication, and match–mismatch) were examined to explain the variability in

jellyfish outbreaks in the YECS. Our results indicated that the long-term increases in *N. nomurai* outbreaks and the recent absence may be driven by anthropogenic factors and climate change (Fig. 10).

Increased eutrophic conditions and the warming of seawater in late spring and early summer were favorable to, and a necessary condition for, the long-term increase in *N. nomurai* outbreaks in JY. However, significantly lower SST in NJY compared with JY indicates that SST was an important factor lowering the proliferation of *N. nomurai* in NJY through effects on survival of ephyra. Timing of phytoplankton blooms varied interannually and spatially, and their match and mismatch to the timing of SST reaching 15°C was not corresponded to the long-term increases in *N. nomurai* outbreaks and the recent absence. Instead, survival of ephyra may differ in middle and coastal areas. Once ephyra establishes its population with high survival rates, the fast growth from ephyra to young medusae under favorable conditions (temperature, food) probably could lead to a later jellyfish outbreak.

Acknowledgments We thank NASA/DAAC for providing AVHRR, SeaWiFS, and MODIS data. We also thank Prof. Shin-ichi Uye for providing valuable advice about the ecology and biology of giant jellyfish. We thank Prof. Egil Sakshaug for scientific and writing support. Two anonymous reviewers and the editor also provided valuable comments on the manuscript. This work was funded by the Fisheries Agency of Japan as the “International Cooperative Study of Giant Jellyfish.”

References

Ahn YH and Shanmugam P (2006) Detecting the red tide algal blooms from satellite ocean color observations in optically complex Northeast-Asia Coastal waters. Remote Sens Environ 103(4):419-437. doi: 10.1016/j.rse.2006.04.007

Båmstedt U, Wild B and Martinussen M (2001) Significance of food type for growth of ephyrae *Aurelia aurita* (Scyphozoa). Mar Biol 139(4):641-650. doi: 10.1007/s002270100623

Beardsley RC, Limeburner R, Yu H, and Cannon GA (1985) Discharge of the Changjiang (Yangtze River) into the East China Sea. Cont Shelf Res 4(1-2): 57-76

Chai CZ, Yu M, Song XX and Cao XH (2006) The Status and Characteristics of Eutrophication in the Yangtze River (Changjiang) Estuary and the Adjacent East China Sea, China. Hydrobiologia 563(1):313-328. doi: 10.1007/s10750-006-0021-7

Cushing DH (1990) Plankton production and year-class strength in fish populations: an update of the match/mismatch hypothesis. Adv Mar Biol 26:249-294. doi: 10.1016/S0065-2881(08)60202-3

Durant JM, Hjermann DO, Anker-Nilssen T, Beaugrand G, Mysterud A, Pettorelli N, and Stenseth NC (2005) Timing and abundance as key mechanisms affecting trophic interactions in variable environments. Ecology Letters 8:952–958. doi: 10.1111/j.1461-0248.2005.00798.x

Frank KT, Petrie B and Shackell NL (2007) The ups and downs of trophic control in continental shelf ecosystems. Trends Ecol Evol 22(5):236–242. doi:10.1016/j.tree.2007.03.002

Furuya K, Hayashi M and Yabushita Y (2003) Phytoplankton dynamics in the East China Sea in spring and summer as revealed by HPLC-derived pigment signatures. Deep Sea Res Part II 50:367-387. doi: 10.1016/S0967-0645(02)00460-5

Gao C and Zhang T (2010) Eutrophication in a Chinese Context: Understanding Various Physical and Socio-Economic Aspects. AMBIO 39(5-6):385-393. doi: 10.1007/s13280-010-0040-5

Gao XL and Song JM (2005) Phytoplankton distributions and their relationship with the environment in the Changjiang Estuary, China. Mar Pollut Bull 50(3):327-335. doi: 10.1016/j.marpolbul.2004.11.004

Gremillet D, Lewis S, Drapeau L, van Der Lingen CD, Huggett JA, Coetzee JC, Verheye HM, Daunt F, Wanless S and Ryan PG (2008) Spatial match-mismatch in the Benguela upwelling zone: should we expect chlorophyll and sea-surface temperature to predict marine predator distributions? J Appl Ecol 45(2):610-621. doi: 10.1111/j.1365-2664.2007.01447.x

Henson SA and Thomas AC (2007) Interannual variability in timing of bloom initiation in the California Current System. J Geophys Res 112(C08007):1-12. doi: 10.1029/2006JC003960

Hickox (2000) Climatology and seasonal variability of ocean fronts in the East China, Yellow and Bohai seas from satellite SST data. Geophys Res Lett (27):2945–2948. doi: 10.1029/1999GL011223

Hu C, Li D, Chen CS, Ge JZ, Muller-Karger FE, Liu JP, Yu F and He MX (2010) On the recurrent Ulva prolifera blooms in the Yellow Sea and East China Sea. J Geophys Res 115:C05017. doi: 10.1029/2009JC005561

Jiao N, Zhang Y and Zeng Y (2007) Ecological anomalies in the East China Sea: Impacts of the Three Gorges Dam? Water Res 41(41):1287-1293. doi: 10.1016/j.watres.2006.11.053

Kang YS, Jung S, Zuenko Y, Choi I, Dolganova N (2012) Regional differences in the response of mesozooplankton to oceanographic regime shifts in the northeast asian marginal seas, Prog Oceanogr, 97:120-134. doi: 10.1016/j.pocean.2011.11.012

Kaufman L and Rousseeuw PJ (1990) Finding Groups In Data: An Introduction to Cluster Analysis, John Wiley & Sons, p 368

Kawahara MS, Uye S, Ohtsu K and Izumi H (2006) Unusual population explosion of the giant jellyfish *Nemopilemia nomurai (Scyphozoa : Rhizostomeae)* in East Asian waters. Mar Ecol Prog Ser 307:161-173. doi:10.3354/meps307161

Kawahara M, Ohtsu K and Uye S (2013) Bloom or non-bloom in the giant jellyfish *Nemopilema nomurai* (Schphozoa: Rhizostomeae): roles of dormant podocysts. J Plankton Res 35(1):213-217. doi:10.1093/plankt/fbs074

Kim HC, Yamaguchi H, Yoo S, Zhu JR, Okamura K, Kiyomoto YK, Tanaka K, Kim SW, Park T, O IS and Ishizaka J (2009) Distribution of Changjiang Diluted Water Detected by Satellite Chlorophyll-a and Its Interannual Variation during 1998–2007. J Oceanogr 65:129-135. doi: 10.1007/s10872-009-0013-0

Kiorboe T and Nielsen TG (1994) Regulation of Zooplankton Biomass and Production in a Temperate, Coastal Ecosystem1. Copepods. Limnol Oceanogr 39(3):493-507.

Lee HE, Yoon WD and Lim D (2008) Description of feeding apparatus and mechanism in *nemopilema nomurai* kishinouye (scyphozoa: rhizostomeae). Ocean Sci J 43(1):61-65. doi: 10.1007/BF03022432

Li MT, Xu K, Watanabe M and Chen Z (2007) Long-term variations in dissolved silicate, nitrogen, and phosphorus flux from the Yangtze River into the East China Sea and impacts on estuarine ecosystem. Estuar Coast Shelf S 71(1-2):3-12. doi: 10.1016/j.ecss.2006.08.013

Lin C, Ning X, Su J, Lin Y and Xu B (2005) Environmental changes and the responses of the ecosystem of the Yellow Sea during 1976–2000. J Mar Sys 55(3-4):223-234. doi: 10.1016/j.jmarsys.2004.08.001

Lynam CP, Hay SJ and Brierley AS (2004) Interannual variability in abundance of North Sea jellyfish and links to the North Atlantic Oscillation. Limnol Oceanogr 49(3):637-643. doi: 10.4319/lo.2004.49.3.0637

Lynam CP, Hay SJ and Brierley AS (2005) Jellyfish abundance and climatic variation: contrasting responses in oceanographically distinct regions of the North Sea, and possible implications for fisheries. J Mar Bio Assoc UK 85:435-450. doi: 10.1017/S0025315405011380

Michael PF and Proschan MA (2010) Wilcoxon-Mann-Whitney or t-test? On assumptions for hypothesis tests and multiple interpretations of decision rules. Statistics Surveys 4:1-39. doi: 10.1214/09-SS051

Minnett PJ, Evans RH, Kearns EJ and Brown OB (2002) Sea-surface temperature measured by the Moderate Resolution Imaging Spectroradiometer (MODIS). IEEE International Geosciences and Remote Sensing Symposium. Toronto, Canada.

Platt T, Sathyendranath S and Fuentes-Yaco C (2007) Biological oceanography and fisheries management: perspective after 10 years. ICES J Mar Sci 64:863-869. doi: 10.1093/icesjms/fsm072

Purcell JE, Uye S and Lo WT (2007) Anthropogenic causes of jellyfish blooms and their direct consequences for humans: a review. Mar Ecol Prog Ser 350:153–174. doi: 10.3354/meps07093

Purcell JE, Hoover RA and Schwarck NT (2009) Interannual variation of strobilation by the scyphozoan *Aurelia labiata* in relation to polyp density, temperature, salinity, and light conditions in situ. Mar Ecol Prog Ser 375:139-149. doi: 10.3354/meps07785

Purcell JE (2012) Jellyfish and Ctenophore Blooms Coincide with Human Proliferations and Environmental Perturbations. Annu Rev Marine Sci 4:209-235. doi: 10.1146/annurev-marine-120709-142751

Richardson AJ, Andrew B, Hays GC and Gibbons MJ (2009) The jellyfish joyride: causes, consequences and management responses to a more gelatinous future. Trends Ecol Evol 24(6):312-322. doi: 10.1016/j.tree.2009.01.010

Siswanto E, Nakata H, Matsuoka Y, Tanaka K, Kiyomoto Y, Okamura K, Zhu JR and Ishizaka J (2008) The long-term freshening and nutrient increases in summer surface water in the northern East China Sea in relation to Changjiang discharge variation. J Geophys Res 113:C10030. doi: 10.1029/2008JC004812

Siswanto E, Tang J and Yamaguchi H, Ahn YH, Ishizaka J, Yoo S, Kim SW, Kiyomoto Y, Yamada K, Chiang C and Kawamura H (2011) Empirical ocean-color algorithms to retrieve chlorophyll-a, total suspended matter, and colored dissolved organic matter absorption coefficient in the Yellow and East China Seas. J Oceanogr 67(5):627-650. doi: 10.1007/s10872-011-0062-z

Sommer U and Lengfellner K (2008) Climate change and the timing, magnitude, and composition of the phytoplankton spring bloom. Global Change Biol 14(6):1199-1208. doi: 10.1111/j.1365-2486.2008.01571.x

Tang DL, Di BP, Wei GF, Ni IH, Oh IS and Wang SF (2006) Spatial, seasonal and species variations of harmful algal blooms in the South Yellow Sea and East China Sea. Hydrobiologia 568(1):245-253. doi: 10.1007/s10750-006-0108-1

Toyokawa M, Shibata M, Cheng JH, Li HY, Ling JZ, Lin N, Liu ZL, Zhang Y, Shimizu M, Akiyama H (2012) First record of wild ephyrae of the giant jellyfish *Nemopilema nomurai*. Fisheries Sci 78(6):1213-1218. doi: 10.1007/s12562-012-0550-0

Uye S (2008) Blooms of the giant jellyfish *Nemopilema nomurai*: a threat to the fisheries sustainability of the East Asian Marginal Seas. Plankton and Benthos Research 3(Suppl):125–131

Uye S (2011) Human forcing of the copepod-fish-jellyfish triangular trophic relationship. Hydrobiologia 666(1):71-83. doi: 10.1007/s10750-010-0208-9

Vantrepotte V and Melin F (2009) Temporal variability of 10-year global SeaWiFS time-series of phytoplankton chlorophyll a concentration. ICES J Mar Sci (66):1547-1556. doi: 10.1093/icesjms/fsp107

Wang B (2006) Cultural eutrophication in the Changjiang (Yangtze River) plume: History and perspective. Estuar Coast Shelf S (69):471-477. doi: 10.1016/j.ecss.2006.05.010

Wang JJ, Tang DL, and Su Y (2010) Winter phytoplankton bloom induced by subsurface upwelling and mixed layer entrainment southwest of Luzon Strait. J Mar Sys 83(3-4):141-149. doi: 10.1016/j.jmarsys.2010.05.006

Yamada K and Ishizaka J (2006) Estimation of interdecadal change of spring bloom timing, in the case of the Japan Sea. Geophys Res Lett 33:L02608. doi: 10.1029/2005GL024792

Yamaguchi H, Kim HC, Son YB, Kim SW, Okamura K, Kiyomoto Y and Ishizaka J (2012) Seasonal and summer interannual variations of SeaWiFS chlorophyll a in the Yellow Sea and East China Sea. Prog Oceanogr 105:22-29. doi: dx.doi.org/10.1016/j.pocean.2012.04.004

Yamaguchi H, Ishizaka J, Siswanto E, Son YB, Yoo S and Kiyomoto Y (2013) Seasonal and spring interannual variations in satellite-observed chlorophyll-a in the Yellow and East China Seas: new datasets with reduced interference from high concentration of resuspended sediment. Cont Shelf Res 59:1-9. doi:10.1016/j.csr.2013.03.009

Yasuda T (2004) On the unusual occurrence of the giant medusa *Nemopilema nomurai* in Japanese waters. Nippon Suisan Gakkaishi (70):380–386 (in Japanese with English abstract)

Zervoudaki S, Nielsen TG and Carstensen J (2009) Seasonal succession and composition of the zooplankton community along an eutrophication and salinity gradient exemplified by Danish waters. J Plankton Res 31(12):1475-1492. doi: 10.1093/plankt/fbp084

Zhang J, Liu SM, Ren JL, Wu Y and Zhang GL (2007) Nutrient gradients from the eutrophic Changjiang (Yangtze River) Estuary to the oligotrophic Kuroshio waters and reevaluation of budgets for the East China Sea Shelf. Prog Oceanogr 74(4):449-478. doi: 10.1016/j.pocean.2007.04.019

Zhai L, Platt T, Tang C, Sathyendranath S and Walls RH (2011) Phytoplankton phenology on the Scotian Shelf. ICES J Mar Sci 68(4):781–791. doi:10.1093/icesjms/fsq175

Zhou M, Shen Z and Yu R (2008) Responses of a coastal phytoplankton community to increased nutrient input from the Changjiang (Yangtze) River. Cont Shelf Res 28:1483-1489. doi: 10.1016/j.csr.2007.02.009

Figure captions

Fig. 1 Bathymetry of the Bohai Sea, Yellow Sea, and East China Sea. Seven 1 × 1° boxes represent areas for SST investigation: the Bohai Sea (BS), the middle of the northern Yellow Sea (MNYS), the Chinese coast of the southern Yellow Sea (CSYS), the coast of the Shangdong Peninsula (CSDP), the middle of the southern Yellow Sea (MSYS), the Korean coast of the southern Yellow Sea (KSYS), and the Changjiang River estuary (CJE).

Fig. 2 Thirteen-year climatology SST data. (**a)** February, (**b)** May, (**c)** August, and (**d)** November represent winter, spring, summer, and autumn, respectively. Lines indicate the isotherm of 15°C SST.

Fig. 3 Interannual variability in monthly SST during spring to summer (March to June) in **(a)** BS, **(b)** MNYS, **(c)** CSYS, **(d)** CSDP, **(e)** MSYS, **(f)** KSYS, and **(g)** CJE. Error bars indicate standard deviations in each box. Black lines indicate the isotherm of 15°C SST. The seven areas are marked in Fig. 1.

Fig. 4 8-day weekly SST time series in PJY, JY, and NJY during spring to summer (March to June) in **(a)** BS, **(b)** MNYS, **(c)** CSYS, **(d)** CSDP, **(e)** MSYS, **(f)** KSYS, and **(g)** CJE. Error bars indicate standard deviations in each box. Black lines indicate the isotherm of 15°C SST. The seven areas are marked in Fig. 1. The corresponding date in ordinary years of the Julian day calendar is shown in the abscissa.

Fig. 5 Spatial distribution of differences between SST in NJY and JY during (**a)** March, (**b)** April, (**c)** May, and (**d)** June. Blue and red colors indicate whether SST in NJY was significantly lower (h = 1, $p < 0.1$) or not (h = 0, $p > 0.1$), respectively, from values in JY.

Fig. 6 (**a)** Spatial distribution of the temporal pattern of Chl-*a*. Blue, green, red, and black represent the winter bloom, spring bloom, summer bloom, and summer decline regions, respectively. The white grids with few valid satellite data were omitted from further study. (**b)** Detailed separation by K-means clustering of spring bloom and summer bloom regions based on geographical and climatological differences in temporal patterns of Chl-*a*. The spring bloom region was separated into the MNYS and MSYS regions, and the summer bloom region was separated into the BS, CSYS, KSYS, and CJE regions. The light-gray region was omitted from further study because of high SST (always near or above 15ºC)

Fig. 7 The 13-year mean Chl-*a* seasonality in regions of the (**a)** winter, (**b)** spring, and (**c)** summer blooms, and **(d)** the summer decline from 1998 to 2010, with means ± standard deviations of the peak, bloom timing, bloom duration, and baseline. Black vertical lines indicate start and end times of the bloom, and thick gray lines indicate the fitted curve. The corresponding date in ordinary years of the Julian day calendar is shown in the abscissa.

Fig. 8 (**a)** Start time, (**b)** end time, (**c)** peak time, (**d)** duration, (**e)** average Chl-*a* during the non-bloom period (non-bloom Chl-*a*), and **(f)** peak Chl-*a* from 13-year mean Chl-*a* data. Summer decline regions in CSDP are excluded (white).

Fig. 9 Interannual variability in phytoplankton blooms and the Tsst15 in **(a)** BS, **(b)** MNYS, **(c)** CSYS, **(d)** CSDP, **(e)** MSYS, **(f)** KSYS, and **(g)** CJE. Black crosses and squares indicate the start time (ST) and end time (ET), respectively, and red triangles indicate the Tsst15. The corresponding date in ordinary years of the Julian day calendar is shown in the abscissa.

Fig. 10 Conceptual diagram of the temporal relationship between jellyfish outbreaks and environmental variables. In periods when jellyfish and phytoplankton biomass overlap or when eutrophication occurs, the larvae will have adequate food and therefore enhanced survival probability. In years when the water temperature is warmer/colder, the jellyfish larvae will have high/low survival rates, leading to a later presence/absence of jellyfish outbreaks. Green indicates phytoplankton biomass; black curved lines indicate jellyfish abundance in PJY, JY, and NJY; red indicates that SST was temporally higher in PJY and JY than in NJY; and blue indicates that SST was lower. Yellow lines indicate the Tsst15.

Table 1 Satellite data used in this study

Satellite data sets	Sensor	Wavelength(nm)	Product	Resolution	Version	Year
SST	AVHRR	-	-	4 km	5.0	1998-2002
	MODIS	-	Level 3	4 km	-	2003-2010
Remote Sensing Reflectance (Rrs)	SeaWiFS	412, 443, 490, 555	GAC Level 2	4 km	R2005.1	1998-2007
	SeaWiFS	412, 443, 490, 555	GAC Level 2	4 km	R2010.0	1998-2010
	SeaWiFS	412, 443, 490, 555	MLAC Level 2	1 km	R2010.0	2002-2004
	MODIS	412, 443, 488, 547	LAC Level 2	1 km	R2009.1	2002-2008
	MODIS	412, 443, 488, 547	LAC Level 2	1 km	R2010.0	2009-2010

Table 2 Interannual variability of non-bloom Chl-*a*, peak Chl-*a*, timings of phytoplankton blooms and Tsst15

Locations	**Chl-*a* pattern**	**Start time**	**End time**	**Non-bloom Chl-*a*** ($mg\ m^{-3}$)	**Peak Chl-*a*** ($mg\ m^{-3}$)	**13 years increasing trend in non-bloom Chl-*a***	**13 years increasing trend in peak Chl-*a***	**Tsst15**
BS	Summer bloom	Early Mar. to early Jun.	Early Oct. to middle Nov.	1.9~3.1	2.5~4.5	55% ($r = 0.884$, $p < 0.05$), with 19% from PJY to JY	80% ($r = 0.882$, $p < 0.05$), with 31% from PJY to JY	Middle to late May, just after start time
MNYS	Spring bloom	Early Jan. to middle Feb.	Early May to late Jun.	1.0~1.7	1.8~3.3	-	-	Late May to early Jun., just before or after end time
CSYS	Summer bloom	from middle May to middle Jul. except 2009	Middle Aug. to late Oct.	1.4~2.1	2.0~3.2	35.8% ($r = 0.831$, $p < 0.05$), with 14% from PJY to JY	60% ($r = 0.55$, $p < 0.05$), with 18% from PJY to JY	Early May to middle May, just before start time except 2009
MSYS	Spring Bloom	Middle Feb. to early Apr.	Early May to late May	0.8~1.1	1.5~2.3	18% ($r = 0.61$, $p < 0.05$), with 4% from PJY to JY	55% ($r = 0.66$, $p < 0.05$), with 8.2% from PJY to JY	Late May to early Jun., just before or after the end time
KSYS	Summer bloom	Early May to late Aug.	Late Sep. to early Dec.	1.5~2.2	2.5~8.6	35.7% ($r = 0.85$, $p < 0.05$), with 14.5% from PJY to JY	38% ($r = 0.75$, $p < 0.05$), with 26% from PJY to JY	Late May to early Jun., just before or after the start time
CJE	Summer bloom	Middle Feb. to early Jun.	Middle Aug. to late Dec.	0.7~1.5	2.0~3.8	9.5% without significant trend, with 5% from PJY to JY	8-10% without significant trend, with 5% from PJY to JY	Middle to late Apr., just after start time except 1998-1999

Figure

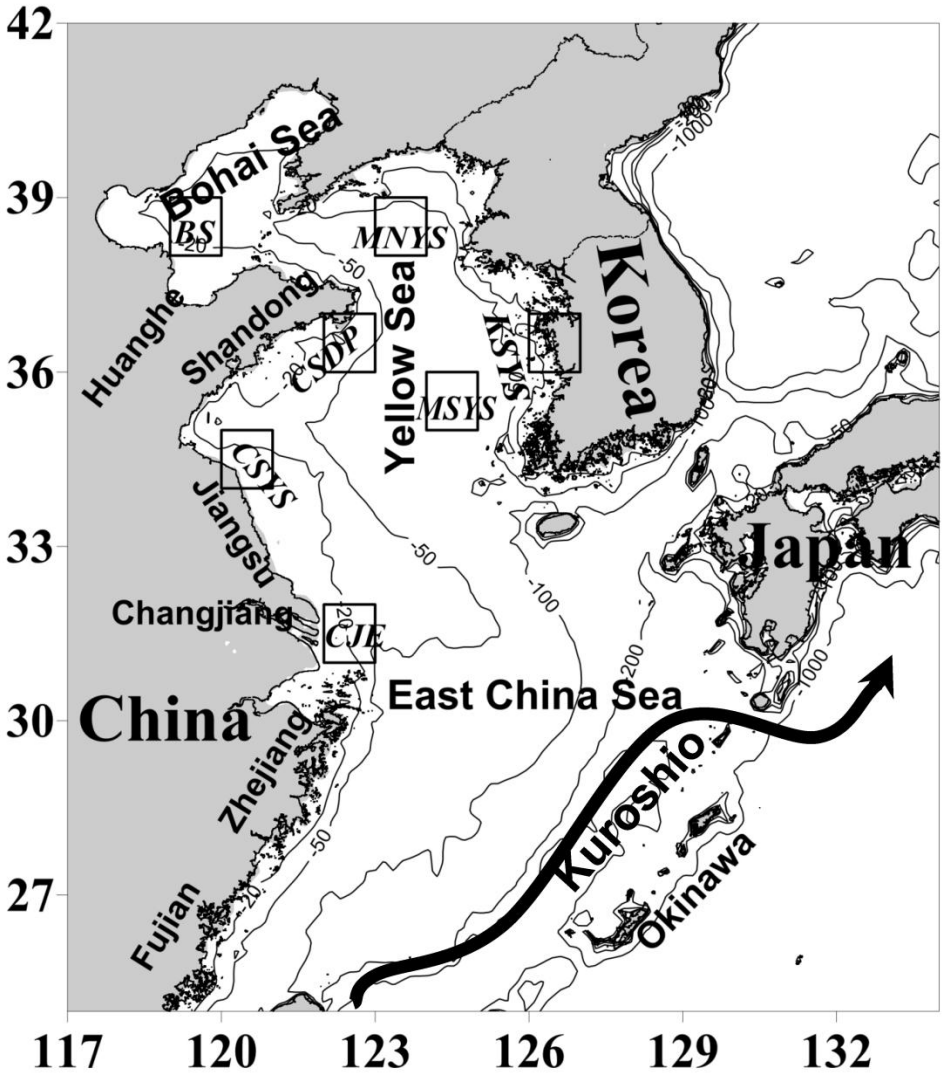
42
39
36
33
30
27
117
120
123
126
129
132
Bohai Sea
BS
MNYS
Yellow Sea
Korea
Huanghe
Shandong
CSDP
KSYS
MSYS
CSYS
Jiangsu
Changjiang
CJE
China
East China Sea
Japan
Zhejiang
Kuroshio
Okinawa
Fujian
-1000
-50
-100
-200

Fig. 1

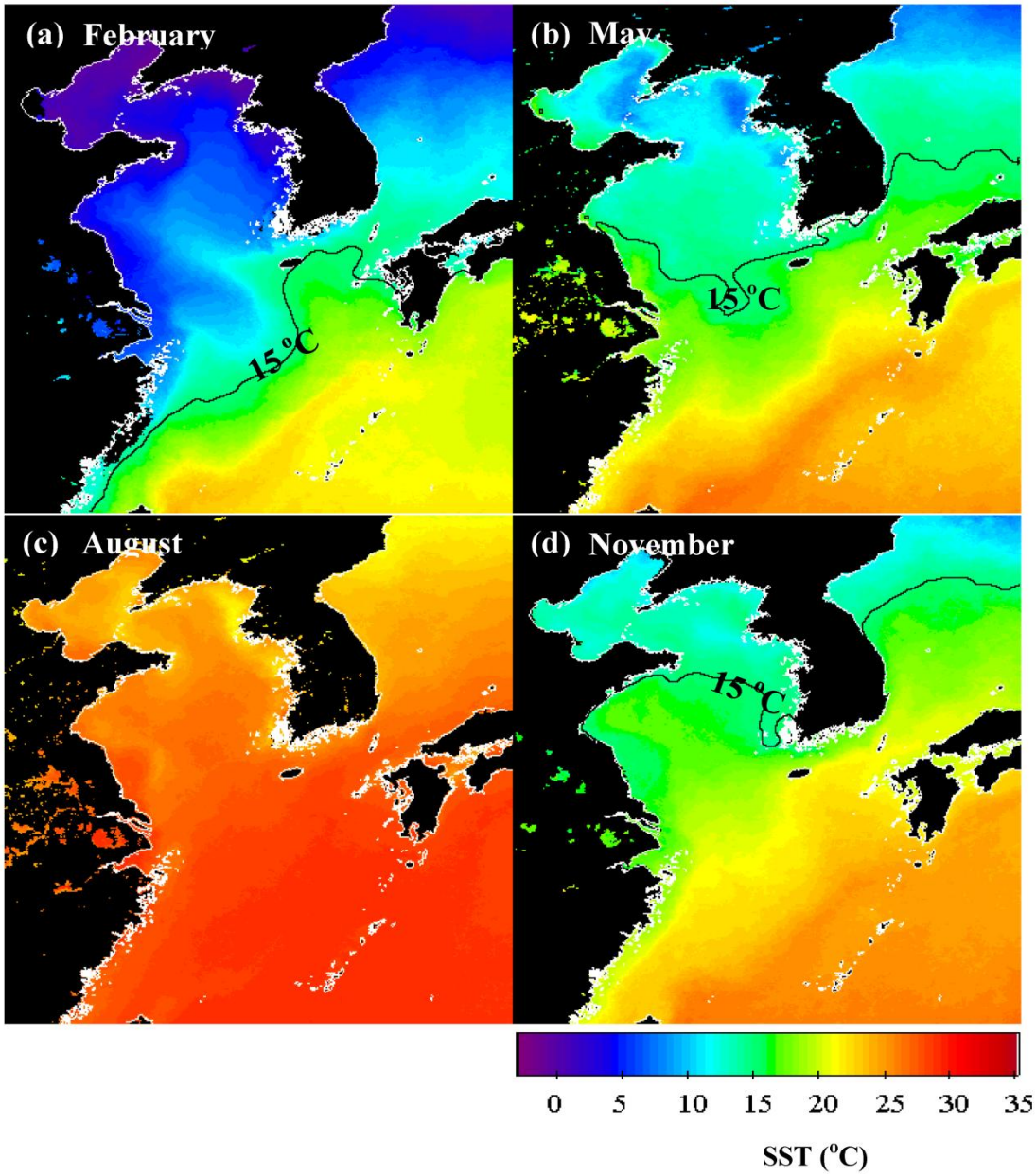
(a) February
15 °C
(b) May
15 °C
(c) August
(d) November
15 °C
0
5
10
15
20
25
30
35
SST (°C)

Fig. 2

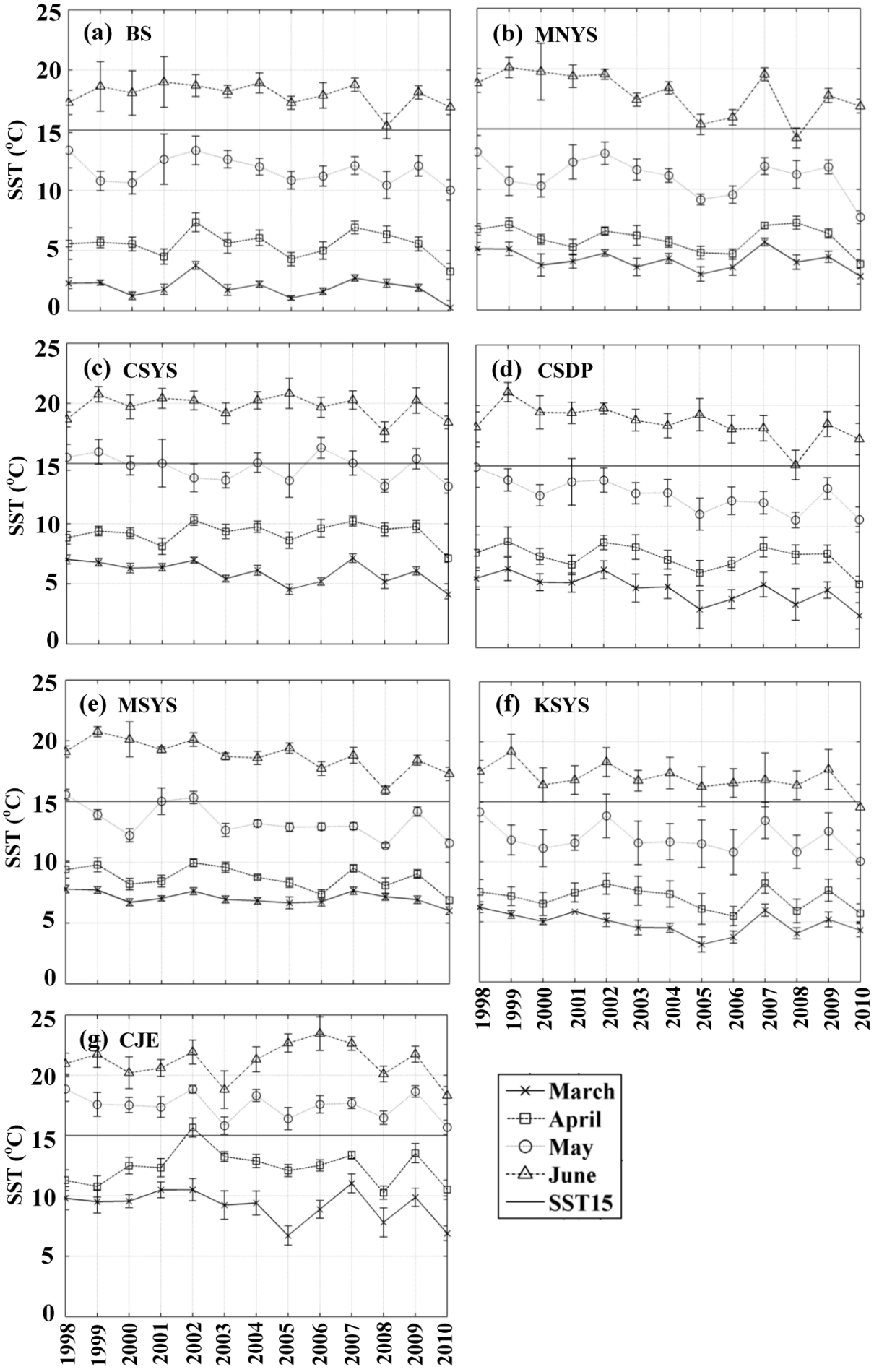
(a) BS
(b) MNYS
(c) CSYS
(d) CSDP
(e) MSYS
(f) KSYS
(g) CJE
SST (°C)
0
5
10
15
20
25
1998
1999
2000
2001
2002
2003
2004
2005
2006
2007
2008
2009
2010
March
April
May
June
SST15

Fig. 3

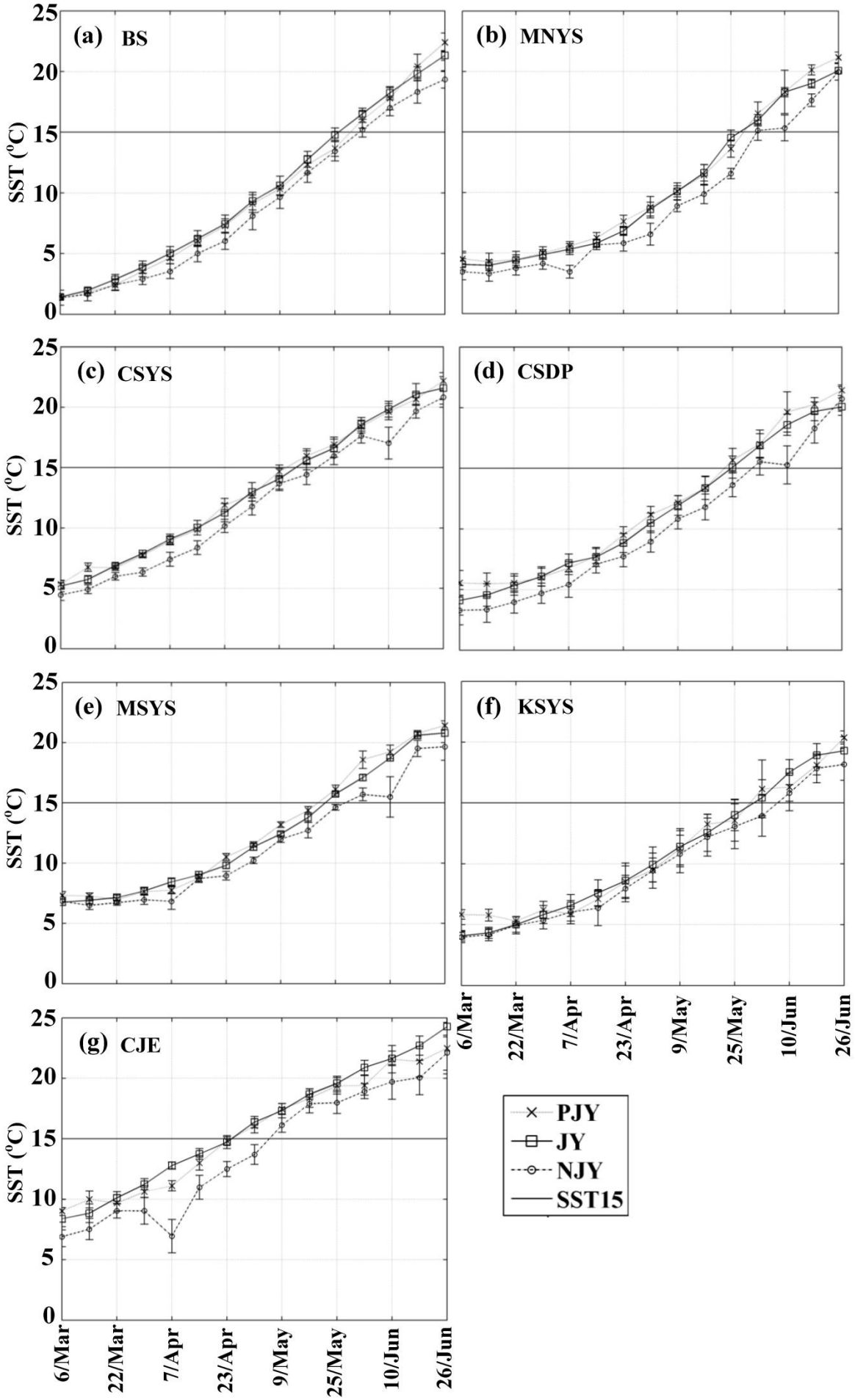
(a) BS
(b) MNYS
(c) CSYS
(d) CSDP
(e) MSYS
(f) KSYS
(g) CJE
SST (°C)
0
5
10
15
20
25
6/Mar
22/Mar
7/Apr
23/Apr
9/May
25/May
10/Jun
26/Jun
PJY
JY
NJY
SST15

Fig. 4

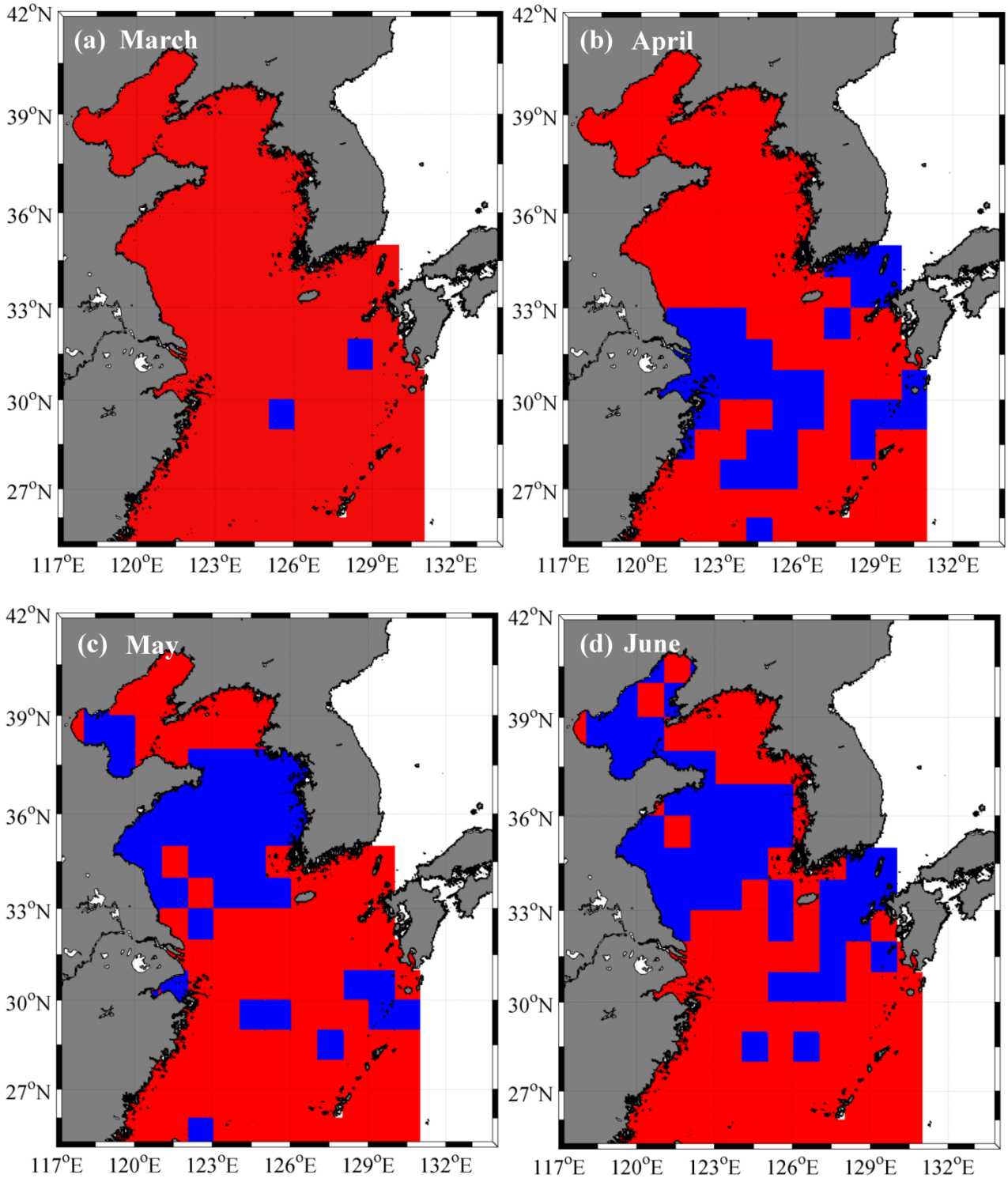
(a) March
(b) April
(c) May
(d) June
42°N
39°N
36°N
33°N
30°N
27°N
117°E
120°E
123°E
126°E
129°E
132°E

Fig. 5

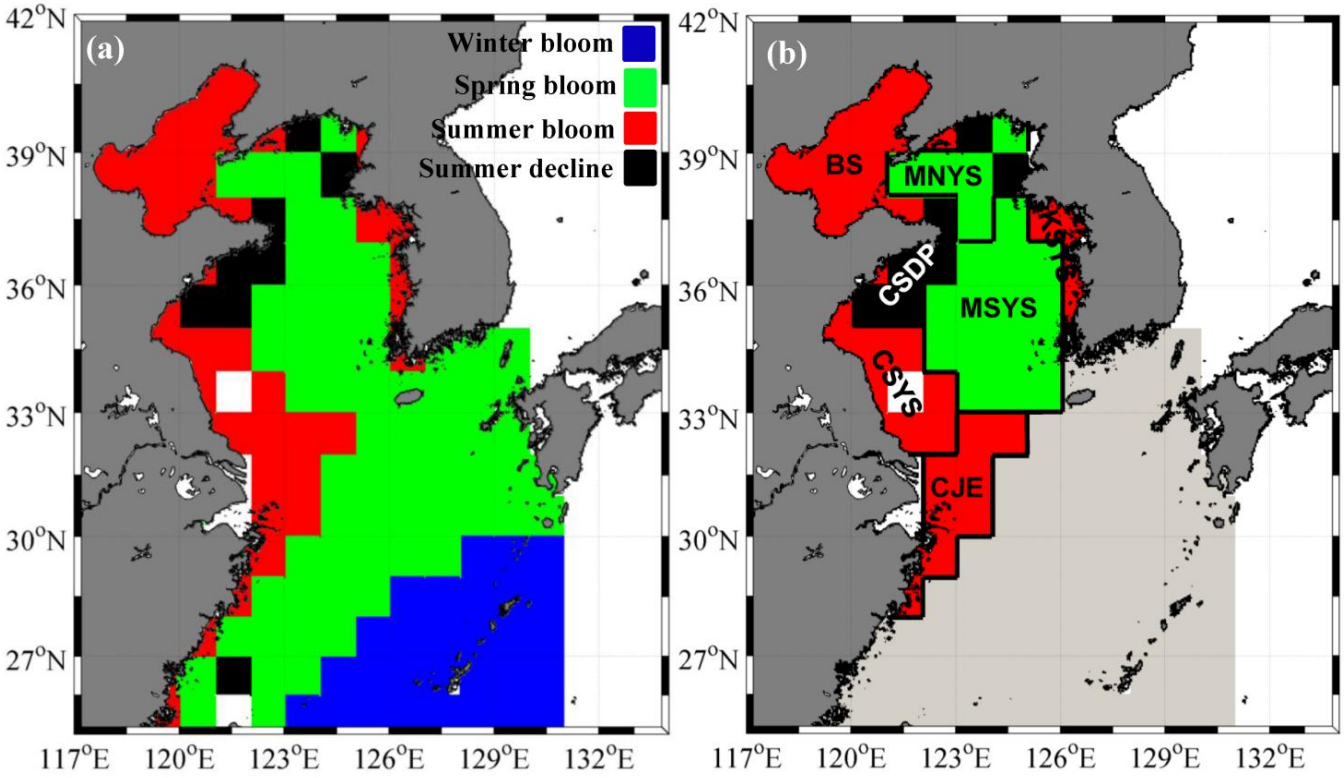
(a)
Winter bloom
Spring bloom
Summer bloom
Summer decline
42°N
39°N
36°N
33°N
30°N
27°N
117°E
120°E
123°E
126°E
129°E
132°E
(b)
BS
MNYS
KSYS
CSDP
MSYS
CSYS
CJE

Fig. 6

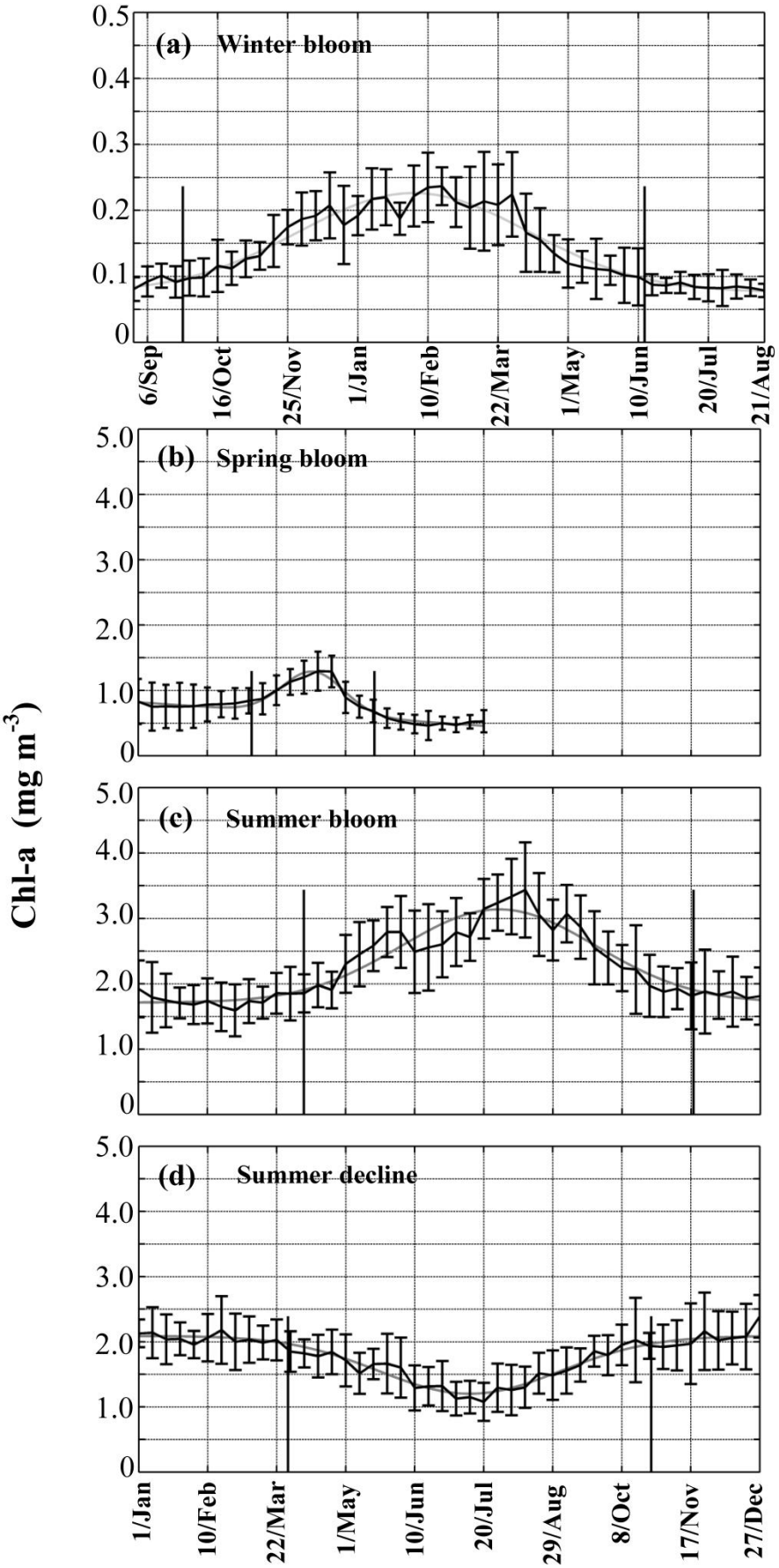
(a) Winter bloom
(b) Spring bloom
(c) Summer bloom
(d) Summer decline
Chl-a (mg m-3)
0.5
0.4
0.3
0.2
0.1
0
5.0
4.0
3.0
2.0
1.0
0
6/Sep
16/Oct
25/Nov
1/Jan
10/Feb
22/Mar
1/May
10/Jun
20/Jul
21/Aug
1/Jan
10/Feb
22/Mar
1/May
10/Jun
20/Jul
29/Aug
8/Oct
17/Nov
27/Dec

Fig.7

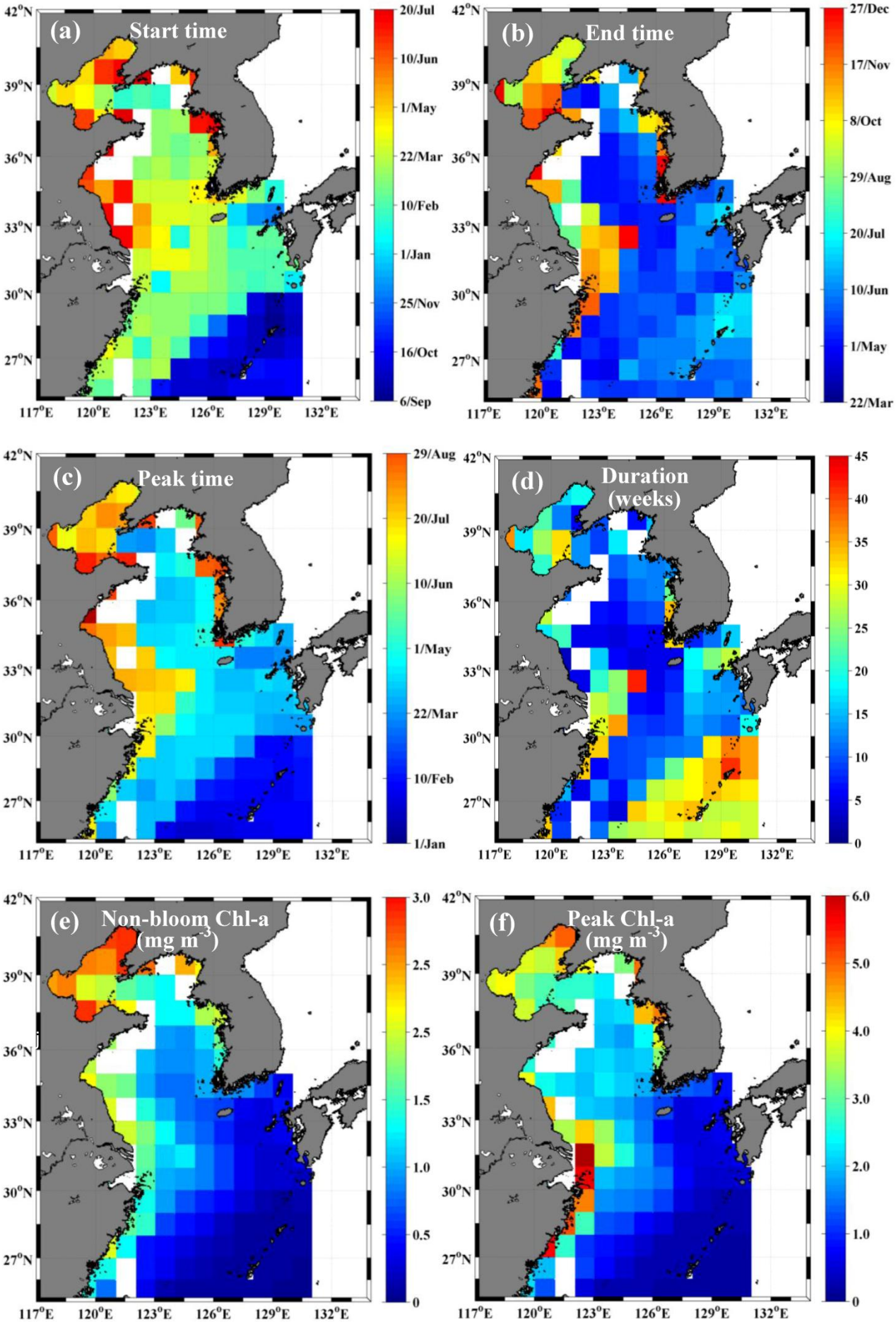
(a) Start time
20/Jul
10/Jun
1/May
22/Mar
10/Feb
1/Jan
25/Nov
16/Oct
6/Sep
(b) End time
27/Dec
17/Nov
8/Oct
29/Aug
20/Jul
10/Jun
1/May
22/Mar
(c) Peak time
29/Aug
20/Jul
10/Jun
1/May
22/Mar
10/Feb
1/Jan
(d) Duration (weeks)
45
40
35
30
25
20
15
10
5
0
(e) Non-bloom Chl-a (mg m-3)
3.0
2.5
2.5
1.5
1.0
0.5
0
(f) Peak Chl-a (mg m-3)
6.0
5.0
4.0
3.0
2.0
1.0
0
42°N
39°N
36°N
33°N
30°N
27°N
117°E
120°E
123°E
126°E
129°E
132°E

Fig. 8

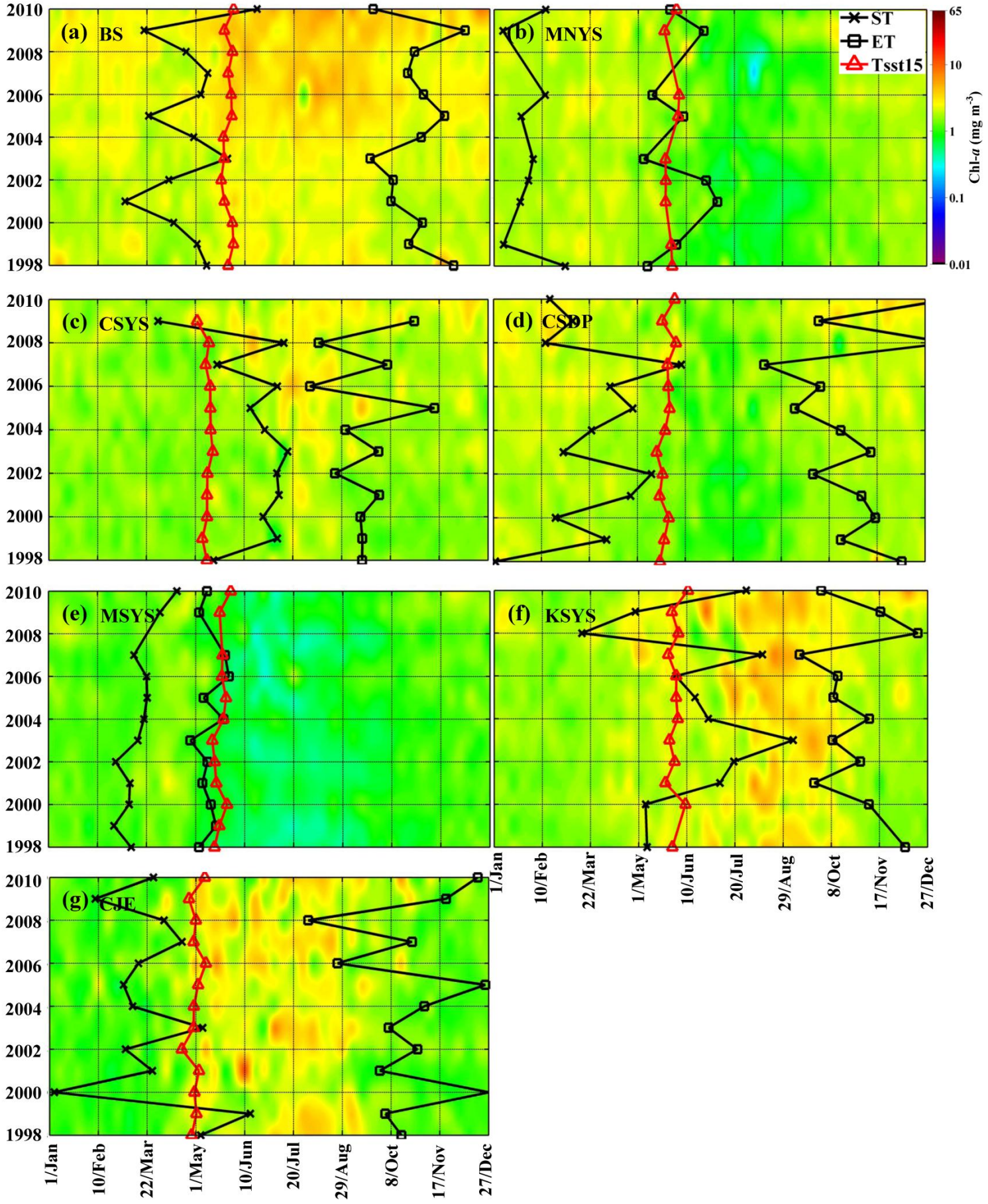
(a) BS
(b) MNYS
(c) CSYS
(d) CSDP
(e) MSYS
(f) KSYS
(g) CJE
ST
ET
Tsst15
Chl-a (mg m-3)
65
10
1
0.1
0.01
2010
2008
2006
2004
2002
2000
1998
1/Jan
10/Feb
22/Mar
1/May
10/Jun
20/Jul
29/Aug
8/Oct
17/Nov
27/Dec

Fig. 9

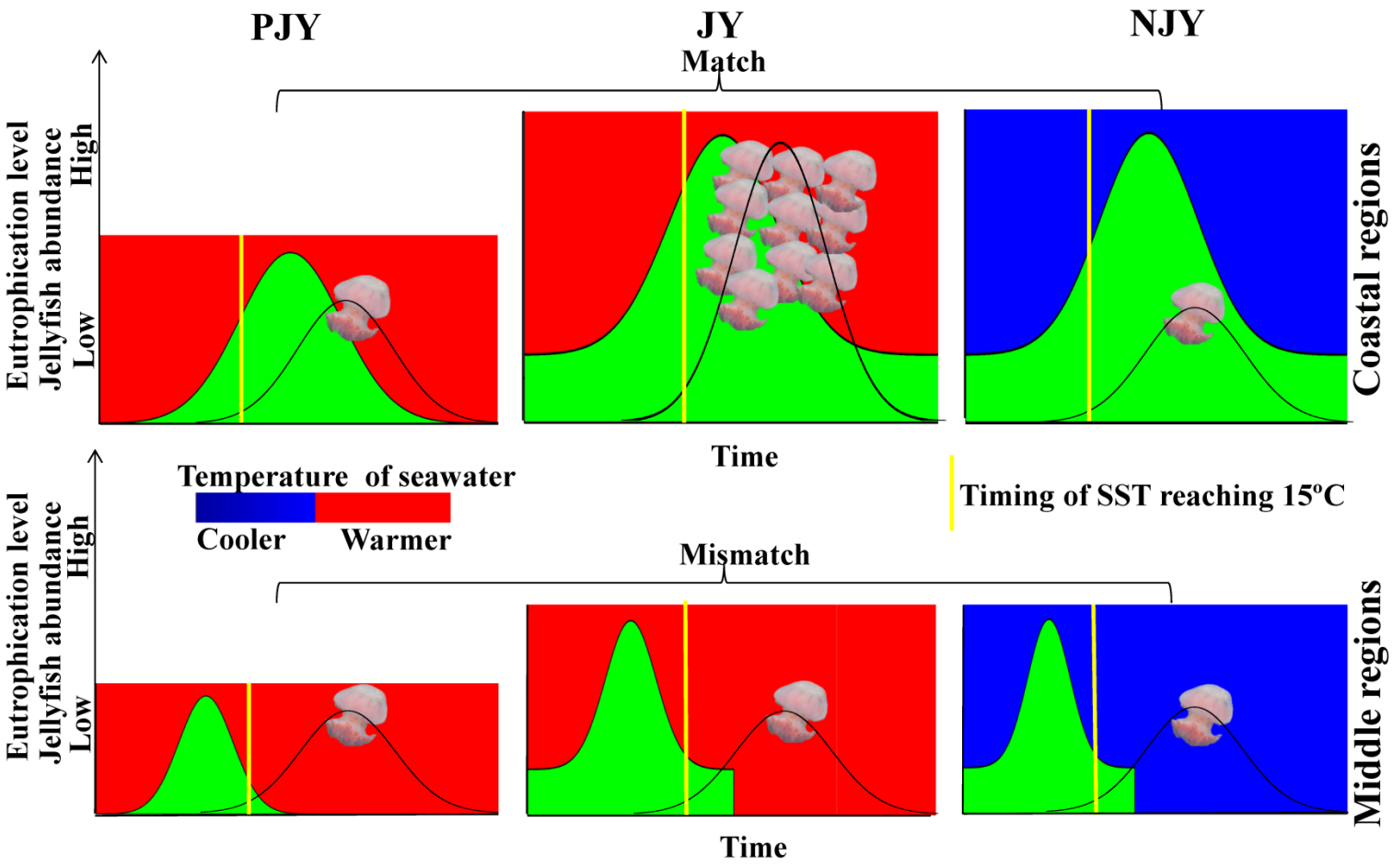
PJY
JY
NJY
Match
Eutrophication level
Jellyfish abundance
High
Low
Coastal regions
Time
Temperature of seawater
Cooler
Warmer
Timing of SST reaching 15°C
Mismatch
Middle regions

Fig. 10

Supplementary Material

Click here to download Supplementary Material: Yongjiu_Xu_Appendix_revision_final_2013_06_18.doc